Journal of Physics: Conference Series **547** (2014) 012022 doi:10.1088/1742-6596/547/1/012022

The thermal entrance region in a porous medium saturated by a nanofluid: analysis of the Brinkman's model

Eugenia Rossi di Schio

Alma Mater Studiorum - Università di Bologna.
Department of Industrial Engineering. Viale Risorgimento 2, 40136 Bologna, Italy

E-mail: eugenia.rossidischio@unibo.it

Abstract. The Darcy-Graetz problem for a channel filled by a nanofluid saturated porous medium is studied. The flow is assumed to be fully developed and described through Brinkman's model. For the model of the nanofluid, both thermophoresis and Brownian diffusion are taken into account. After an adiabatic preparation region, a boundary temperature linearly varying with the longitudinal coordinate is prescribed. A study of the thermal behaviour of the nanofluid is performed by solving numerically the fully–elliptic coupled equations, with reference both to the thermal entrance region and to the fully developed region. With reference to the fully developed region the solution has been obtained analytically, while for the thermal entrance region it has been obtained numerically, by a Galerkin finite element method implemented through the software package Comsol Multiphysics (© Comsol, Inc.). The analysis shows that, for physically interesting values of the Péclet number, the concentration field depends very weakly on the temperature distribution, for any given value assumed by the Darcy number. Indeed, since the effects of thermophoresis and Brownian diffusion are negligible, the homogeneous model could be employed effectively.

1. Introduction

As is well known, a nanofluid, i.e. a suspension of nanoparticles in a base fluid, is an innovative technique that uses ultra fine solid particles in the fluid to improve the heat transfer occurring in industrial and technology applications like power manifacturing, transportation, electronics, etc [1–4]. A comprehensive survey of convective transport in nanofluids was made by Buongiorno [5] and Kakaç and Pramuanjaroenkij [6].

Recently, the topic of heat transfer in nanofluids has been deeply investigated [7–15]. Two different approaches can be distinguished in order to model the nanofluid behaviour: one may consider the distribution of the nanoparticles in the base fluid as homogeneous or may consider the distribution of nanoparticles in the base fluid as non-homogeneous. These two different approaches lead to different sets of governing equations: the homogeneous model is totally equivalent to the model employed for clear fluids except for a suitable rescaling of the governing parameters due to the presence of nanoparticles inside the base fluid [11]. Among all possible homogeneous models, an example is that defined by Tiwari and Das [12]. A non-homogeneous model, on the other hand, adds one or more equations to the set of governing equations in order to describe the nanoparticle distribution and/or the nanoparticle velocity. Among the

possible non-homogeneous models, the most widely employed is the model by Buongiorno [5], a model suitable for the heat transfer analysis and for the investigation of the nonhomogeneous distributions of nanoparticles. In this paper, the set of local balance equations appropriate for the study of the flow of nanofluids is presented, with an emphasis on the physical effects peculiar for nanofluids: thermophoresis and Brownian diffusion.
According to the author's knowledge, despite the growing amount of studies dealing with nanofluid saturated porous media, very few papers analyze the forced convection. In particular, the problem is treated by means of Buongiorno's model by Nield and Kuznetsov [14], and by means of the alternative approach of considering the porous medium as composed by an array of microchannels by Hung [15].
The Graetz-like problems, namely the problems dealing with the thermal entrance region in a channel or a duct, have been widely investigated. The aim of the present contribution is to extend the analysis presented in [13] for a clear nanofluid to the special case of a nanofluid saturating a porous medium.
In the present contribution, we aim to investigate the steady laminar forced convection in a parallel-plane channel, filledy by a nanofluid saturated porous medium.

2. Mathematical model

We consider a channel bounded by two impermeable plates having distance $2L$, and infinite longitudinal length. Due to the symmetry, the problem is two-dimensional: let $\overline{x}$ be the longitudinal coordinate, while $\overline{y}$ is the transverse one. The flow is assumed to be fully developed, according to Brinkman law. We refer to the nanofluid model introduced by Buongiorno [5]. The thermal entrance region is studied assuming an adiabatic preparation of the duct [13] upstream of the thermal entrance region, where a boundary temperature varying with the longitudinal coordinate is prescribed. For the nanoparticle concentration, an inlet condition given by a uniform distribution is assumed while the boundary walls are considered as impermeable. Downstream of the adiabatic preparation region, a boundary temperature given by a linear function of the longitudinal coordinate is prescribed. The aim of this paper is to solve the fully elliptic coupled equations, for the temperature and concentration fields. First, the temperature and concentration fields are determined analytically. Then, the numerical solution for the thermal entrance region is obtained by a Galerkin finite element method implemented through the software package Comsol Multiphysics.
In the hydrodynamically developed region, the assumptions imply that the velocity is parallel to the axial direction $\overline{x}$, namely

$$U = \overline{\Lambda} L\, U_m \frac{\cosh(\overline{\Lambda} L) - \cosh(\overline{\Lambda}\overline{y})}{\overline{\Lambda} L \cosh(\overline{\Lambda} L) - \sinh(\overline{\Lambda} L)}, \tag{1}$$

where U_m is the man value of the velocity distribution and

$$\overline{\Lambda} = \sqrt{\frac{\mu}{K\,\mu'}}\ , \tag{2}$$

with K permeability of the porous medium, μ viscosity and μ' effective viscosity of the porous medium. By invoking that local thermal equilibrium holds, the diffusion equation for the nanoparticles and the local energy balance equation for the fluid are given by

$$U\frac{\partial \tilde{\phi}}{\partial \overline{x}} = \varepsilon \overline{\boldsymbol{\nabla}} \cdot \left(D_B \overline{\boldsymbol{\nabla}} \tilde{\phi} + D_T \frac{\overline{\boldsymbol{\nabla}} T}{\overline{T}} \right), \tag{3}$$

$$U\frac{\partial \overline{T}}{\partial \overline{x}} = \alpha_m \overline{\nabla}^2 \overline{T} + \tau \left(D_B \overline{\boldsymbol{\nabla}} \tilde{\phi} \cdot \overline{\boldsymbol{\nabla} T} + D_T \frac{\overline{\boldsymbol{\nabla} T} \cdot \overline{\boldsymbol{\nabla} T}}{\overline{T}} \right), \tag{4}$$

where

$$\alpha_m = \frac{k_m}{(\varrho c)_f}, \quad \tau = \frac{\varepsilon(\varrho c)_{np}}{(\varrho c)_f}. \tag{5}$$

In Eqs. (3) and (4) ε is the porosity of the porous medium, $\tilde{\phi}$ is the nanoparticle concentration, $\overline{T}$ is the temperature, D_B and D_T are the Brownian diffusion and the thermophoresis coefficients, defined as

$$D_B = \frac{k_B\, T_i}{3\,\pi\,\mu\, d_P}, \qquad D_T = \beta\,\nu\,\phi_0, \tag{6}$$

and β is a proportionality factor defined by McNab and Meisen [16].
The thermal boundary conditions can be described as follows: at the inlet section the fluid temperature is uniform and denoted as T_i; then, after an adiabatic preparation, the wall temperature assumes the value T_w at $\overline{x} = 0$ and starts changing linearly in the longitudinal direction, namely

$$\overline{T}(\overline{x}, \pm L) = T_w + (T_w - T_i)\frac{\overline{x}}{L}. \tag{7}$$

Let us introduce the following dimensionless quantities:

$$\begin{aligned} &x = \frac{\overline{x}}{L}\ ,\ y = \frac{\overline{y}}{L}\ ,\ u = \frac{U}{U_m}\ ,\ T = \frac{\overline{T}}{T_i}\ ,\ N_{BT} = \frac{D_B\,\phi_0}{D_T}\ , \\ &Le = \frac{\alpha_m}{\varepsilon D_B}\ ,\ Pe = \frac{U_0\, L}{\alpha_m}\ ,\ G = \frac{\phi_0(\varrho c)_{np}}{(\varrho c)_f}\ ,\ \gamma = \frac{T_w}{T_i}\ ,\ \Lambda = \overline{\Lambda} L\ , \end{aligned} \tag{8}$$

where Le is the Lewis number and Λ is Darcy number. As is well known, Darcy number usually assumes very small values compared with unity in highly porous media. According to the bridging role of Brinkman model, the limit $\Lambda \to 0$ yields to Darcy law, while the limit $\Lambda \to \infty$ yields to the clear fluid behavior, thus allowing a qualitative comparison with the results presented in [13].
Moreover, let us rescale the volumetric fraction of nanoparticle with respect to the inlet value, i.e.

$$\phi = \frac{\tilde{\phi}}{\phi_0}. \tag{9}$$

By employing the dimensionless quantities, Eqs. (1), (3) and (4) can be rewritten as

$$u = \Lambda \frac{\cosh(\Lambda) - \cosh(\Lambda\, y)}{\Lambda\cosh(\Lambda) - \sinh(\Lambda)}, \tag{10}$$

$$u\frac{\partial \phi}{\partial x} = \frac{1}{Le\, Pe}\left[\nabla^2\phi + \frac{1}{N_{BT}}\left(\frac{\nabla^2 T}{T} - \frac{\boldsymbol{\nabla} T\cdot\boldsymbol{\nabla} T}{T^2}\right)\right], \tag{11}$$

$$u\frac{\partial T}{\partial x} = \frac{\nabla^2 T}{Pe} + \frac{G}{Le\, Pe}\left(\boldsymbol{\nabla}\phi\cdot\boldsymbol{\nabla} T + \frac{1}{N_{BT}}\frac{\boldsymbol{\nabla} T\cdot\boldsymbol{\nabla} T}{\overline{T}}\right), \tag{12}$$

to be solved together with the dimensionless boundary conditions,

$$T(x, \pm 1) = \gamma + x(\gamma - 1). \tag{13}$$

In order to evaluate the order of magnitude of the dimensionless parameters, we refer to typical values of the thermophysical properties for water and copper flowing in a porous medium with porosity 0.5. Of course, the parametric analysis allows a different choice of the values. One may

now choose the typical size of the nanoparticle $d_p \approx 10^{-9}$m and an inlet volumetric fraction of the nanoparticle $\phi_0 \approx 10^{-2}$. According to this choice, the values of N_{BT}, Le and G become

$$N_{BT} = 0.46 \ , \ \ Le = 1.7 \cdot 10^4 \ , \ \ G = 8.61 \cdot 10^{-3}. \tag{14}$$

Eq. (14) shows that the fraction G/Le that appears in Eq. (12) is of order of magnitude 10^{-7}, and this justifies neglecting the last term on the right hand side of Eq. (12). Equation (12) thus becomes

$$u\frac{\partial T}{\partial x} = \frac{\nabla^2 T}{Pe}. \tag{15}$$

Eq. (15), together with the boundary conditions, shows that the dimensionless temperature depends only on the parameters Pe and Λ and on the boundary condition, i.e. Eq. (13), and namely on the parameter γ. On the contrary, Eq. (11) shows that the distribution of the volumetric fraction of the nanoparticles is influenced by the temperature field as well.
One can introduce the following dimensionless temperature,

$$\tilde{T} = \frac{\overline{T} - T_i}{T_w - T_i} = \frac{T - 1}{\gamma - 1}. \tag{16}$$

By employing Eq. (16), Eq. (15) becomes

$$u\frac{\partial \tilde{T}}{\partial x} = \frac{\nabla^2 \tilde{T}}{Pe}. \tag{17}$$

to be solved together with the inlet condition, $\tilde{T} = 0$, and with the boundary conditions,

$$\begin{aligned} &\frac{\partial \tilde{T}}{\partial y} = 0, \ \ \text{for} \ \ x < 0, \ y = \pm 1; \\ &\tilde{T} = 1 + x \ \ \text{for} \ \ x \geq 0, \ y = \pm 1. \end{aligned} \tag{18}$$

Eqs. (17) and (18) show that the dimensionless temperature $\tilde{T}$ does not depend on the parameter γ.

2.1. Fully developed region
Let us first investigate the region far from the entrance region, where the solution of Eq. (15), together with the boundary conditions (13), can be obtained analytically. The analytical solution obtained for the fully developed region will be employed to determine the dimensionless functions to be prescribed on the outlet section, in order to investigate the thermal entrance region.
One may assume that, far from the entrance region, the dimensionless temperature distribution is given by the sum of a linear function of the longitudinal coordinate and a function of the transverse coordinate, namely

$$T(x, y) = \gamma + x(\gamma - 1) + \Theta(y). \tag{19}$$

By substituting Eq. (19) into Eq. (15), and by employing Eq. (10), one has

$$\frac{\mathrm{d}^2\Theta}{\mathrm{d}y^2} = (\gamma - 1)Pe\,\Lambda\frac{\cosh(\Lambda) - \cosh(\Lambda\, y)}{\Lambda\cosh(\Lambda) - \sinh(\Lambda)}, \tag{20}$$

to be solved together with the boundary condition $\Theta(y) = 0$ for $y = \pm 1$. Indeed, one obtains

$$\Theta(y) = \frac{(\gamma - 1)Pe}{2\Lambda} \ \frac{\left[2 + \Lambda^2\left(y^2 - 1\right)\right]\cosh(\Lambda) - 2\cosh(\Lambda y)}{\Lambda\cosh(\Lambda) - \sinh(\Lambda)}. \tag{21}$$

With reference to the concentration, in the fully developed region, the temperature gradient in the longitudinal direction remains constant while the dimensionless temperature increases with the longitudinal coordinate, thus allowing us to infer that the last terms on the righthand side of Eq. (11) can be dropped. Indeed, far from the thermal entrance region, the governing equation for the concentration becomes

$$u\frac{\partial\phi}{\partial x} = \frac{\nabla^2\phi}{Le\,Pe}. \tag{22}$$

Similarly, one can infer that the boundary condition for the nanoparticle concentration becomes

$$\left.\frac{\partial\phi}{\partial y}\right|_{y=\pm1} = 0. \tag{23}$$

Indeed, one may assume that, far from the entrance region, the nanoparticle concentration distribution is given by the sum of a linear function of the longitudinal coordinate and a function of the transverse coordinate, namely

$$\phi(x,y) = A\,x + \Phi(y). \tag{24}$$

By substituting Eq. (24) into Eq. (22), one has

$$Le\,Pe\,A\,\Lambda\frac{\cosh(\Lambda)-\cosh(\Lambda\,y)}{\Lambda\cosh(\Lambda)-\sinh(\Lambda)} = \frac{\mathrm{d}^2\Phi}{\mathrm{d}y^2}, \tag{25}$$

to be solved together with the boundary condition (23). By integrating Eq.(25) with respect to y in the interval $[-1,1]$, and by employing Eq.(23), one obtains

$$A = 0 \;\;,\;\; \Phi = const. \tag{26}$$

Equations (21), (24) and (26) yield the dimensionless temperature and concentration distributions to be prescribed on the outlet section in the numerical solution for the thermal entrance region.

2.2. Thermal entrance region

The governing equations (11) and (15), together with the dimensionless boundary conditions (13) and (23), have been numerically solved by employing Galerkin's finite element method, implemented through the software package Comsol Multiphysics. The numerical simulations have been performed by considering a half-channel, i.e. $0 \le y \le 1$, and by replacing the boundary conditions in $y = -1$ with the symmetry conditions in $y = 0$, namely

$$\frac{\partial T}{\partial y} = \frac{\partial\phi}{\partial y} = 0. \tag{27}$$

The numerical simulations have been performed by taking into account Eq. (14) and for different values assumed by the parameters Pe, γ and Λ. In particular, the values $Pe = 0.1$ and $Pe = 0.01$, $\gamma = 1.01$ and $\gamma = 1.001$, $\Lambda = 0.1$ and $\Lambda = 10$ have been considered. If reference is made to copper particles suspended in water flowing in a channel with $L = 1\,mm$, then $Pe = 0.01$ corresponds to a mean velocity proportional to 1 mm/s. Moreover, on account of the definition of the dimensionless parameters, the value $\gamma = 1.01$ corresponds, if an inlet temperature of 300 K is assumed, to a boundary temperature of 303 K prescribed at the thermal entrance section, $x = 0$, and then to a boundary temperature increase of 10 K per millimeter of axial length of the channel.

First, the solution has been checked to be independent of the dimensionless length of the

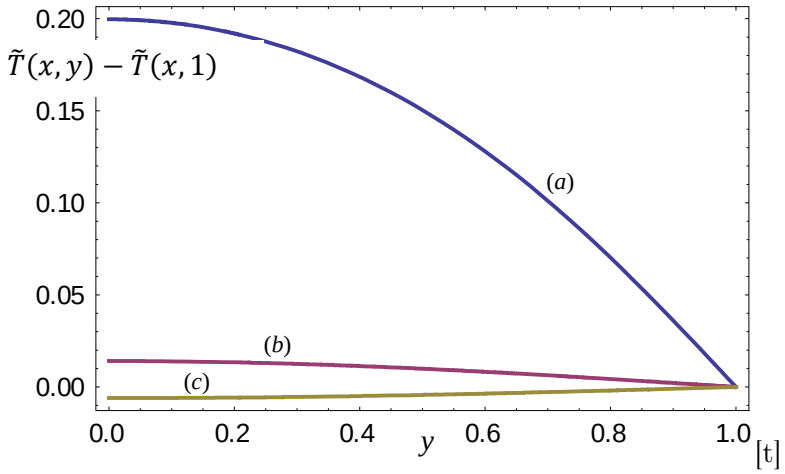

Figure 1. Difference between the dimensionless temperature and the boundary temperature distribution in a half channel for $\Lambda = 0.1$ and $Pe = 0.01$, evaluated at three different axial positions: $x = 0.5$ (a), $x = 2$ (b) and $x = 5$ (c).

computational domain, as well as of the mesh employed. First, different lengths of the thermal entrance region have been compared in the range $10 \leq x_{out} \leq 40$, where x_{out} denotes the dimensionless axial position of the outlet section. In order to perform this comparison, an unstructured mesh of triangular elements has been generated by fixing the maximum element size $m.e.s. = 0.05$. According to this choice, one has, for instance, a mesh consisting of 20100 elements when $x_{out} = 10$; obviously, for increasing lengths of the computational domain, the number of elements increases. Both the cases $Pe = 0.1$ and $Pe = 0.01$ have been tested, assuming $\Lambda = 0.1$. Then, in order to test the independence from the maximum element size, reference has been made to $\gamma = 1.01$ and to the computational domain $-10 \leq x \leq 10$, where $x = 0$ corresponds to the thermal entrance section and $x = -10$ corresponds to the inlet section. The value $\Lambda = 0.1$ has been considered, and both the cases $Pe = 0.1$ and $Pe = 0.01$ have been tested, and different values of the maximum element size have been prescribed, in order to obtain different unstructured meshes characterized by a uniform distribution of triangular elements. The numerical solution has been proved to be independent of the mesh, especially with reference to the axial positions far from the thermal entrance region.

3. Discussion of the results

In this section, the main features of the numerical solution for the thermal entrance region will be discussed. In the present analysis, as explained in the previous section, the values of the parameters given by Eq. (14) have been assumed and a dimensionless axial position of the outlet section $x_{out} = 10$ has been used to define the computational domain. Moreover, an unstructured mesh of triangular elements with maximum element size 0.04 is employed. With reference to the parameters Pe, γ, and Λ different values have been taken into account in order to better investigate the features of the mathematical model.

In Figs. 1 and 2 the difference between the dimensionless temperature distribution $\tilde{T}$ and its value at the boundary is reported, in the thermal entrance region, versus the transverse coordinate y for three different axial positions x and for $Pe = 0.01$. Fig. 1 refers to $\Lambda = 0.1$, while Fig. 2 refers to $\Lambda = 10$. The figures show that far from the thermal entrance region, the temperature distribution tends to become independent of the transverse coordinate y and that this behaviour is reached very soon. Moreover, a comparison between the two figures shows that the solution is

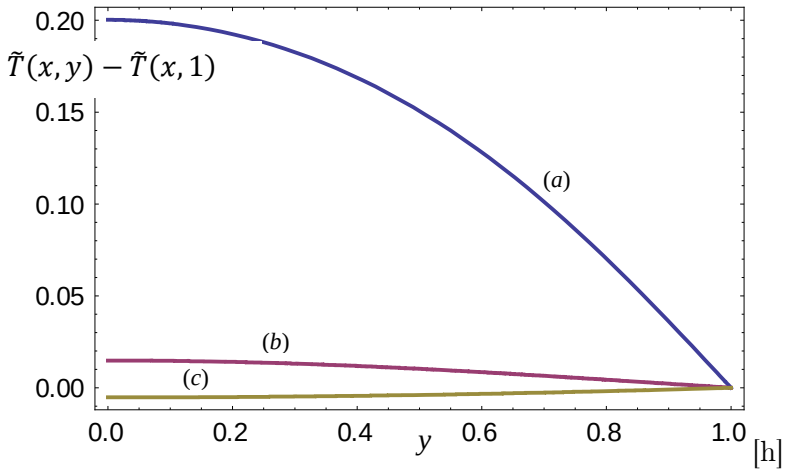

Figure 2. Difference between the dimensionless temperature and the boundary temperature distribution in a half channel for $\Lambda = 10$ and $Pe = 0.01$, evaluated at three different axial positions: $x = 0.5$ (a), $x = 2$ (b) and $x = 5$ (c).

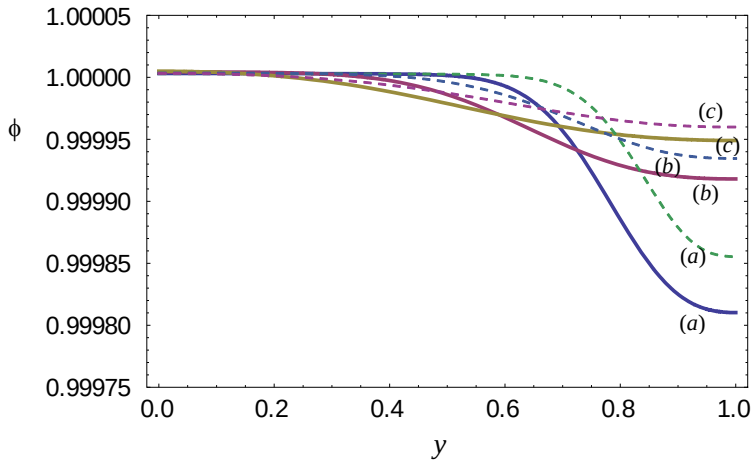

Figure 3. Nanoparticle concentration distribution in a half channel for $Pe = 0.01$ and $\gamma = 1.01$, evaluated at three different axial positions: $x = 0.5$ (a), $x = 2$ (b) and $x = 5$ (c). The solid lines refer to $\Lambda = 10$, while the dashed ones refer to $\Lambda = 0.1$.

not appreciably affected by the velocity distribution, i.e. by the parameter Λ. To underline this feature the unphysical value $\Lambda = 10$ has been assumed in Fig. 2.
In Figs. 3 and 4 the volumetric nanoparticle concentration is reported versus the transverse coordinate y for different axial positions x and for $Pe = 0.01$. Figure 3 refers to $\gamma = 1.01$, while Figure 4 refers to $\gamma = 1.001$. The figures show that the volumetric concentration of nanoparticle varies with the transverse coordinate only in a narrow region close to the boundary of the channel. Moreover, the variability becomes smaller for increasing values of the parameter Λ. However, if one looks at the range of values of the variability of ϕ, one discovers that this range is, indeed, extremely small. The results presented show that the volumetric concentration of nanoparticle is not much affected by the velocity distribution, since it depende very weakly on the parameter Λ, and is not much affected by the temperature distribution, since it depends very weakly on

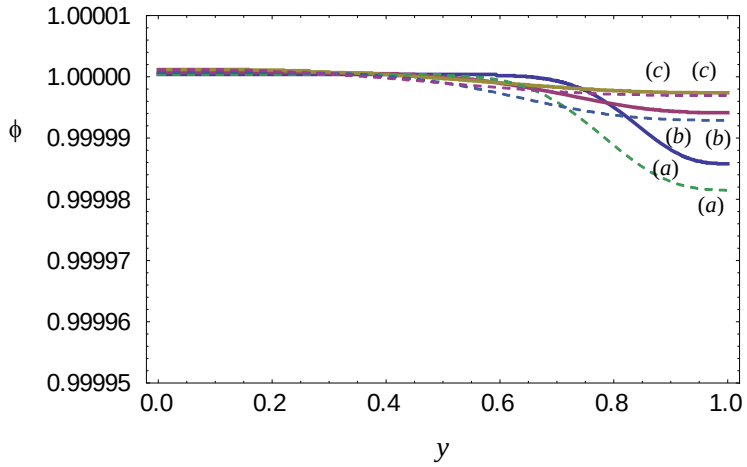

Figure 4. Nanoparticle concentration distribution in a half channel for $Pe = 0.01$ and $\gamma = 1.001$, evaluated at three different axial positions: $x = 0.5$ (a), $x = 2$ (b) and $x = 5$ (c). The solid lines refer to $\Lambda = 10$, while the dashed ones refer to $\Lambda = 0.1$.

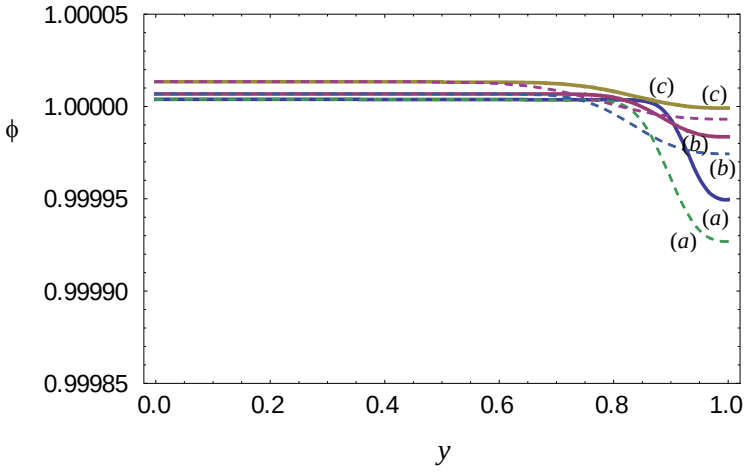

Figure 5. Nanoparticle concentration distribution in a half channel for $Pe = 0.1$ and $\gamma = 1.01$, evaluated at three different axial positions: $x = 0.5$ (a), $x = 2$ (b) and $x = 5$ (c). The solid lines refer to $\Lambda = 10$, while the dashed ones refer to $\Lambda = 0.1$.

the parameters γ and Pe. Moreover, as discussed at the beginning of this section, the value $\gamma = 1.01$ (Fig. 3) is a barely interesting case, since it implies that, if an inlet temperature of 300 K is assumed, the boundary temperature increases 10 K per millimeter along the channel. But the range of values of the variability of ϕ is even smaller for $\gamma = 1.001$, as shown in Fig. 3. In Figs. 3 and 4, the dashed lines refer to the limit of a clear nanofluid, and the results repeat that presented in [13]. Only a qualitative comparison with the results regarding the clear fluid and presented in [13] can be done, since the definition of the dimensionless parameters slightly differs.

Finally, it should be pointed out that Figs. 3 and 4 refer to $Pe = 0.01$. For higher values of the Péclet number the distribution of the nanoparticle concentration depends more on the dimensionless temperature field, but always within a negligicle range of variability. For instance,

results of the nanoparticle concentration referring to $Pe = 0.1$ are reported in Fig. 5, and higher values of Pe are less interesting under a physical point of view.
To sum up, the resolution of the fully-elliptic coupled equations, which arise from the model proposed by Buongiorno [5], requires a computational effort and yields to the determination of a field, the nanoparticle concentration distribution, which may be considered as uniform in many cases of practical interest. Recently, many authors have proposed to consider the nanofluid not through the complete model, but as a normal fluid with properly defined thermophysical properties, i.e. the so-called homogeneous nanofluid model (see, for instance, [11] and [12]). The results arising from the present paper suggest to neglect the nanoparticle concentration gradient, and to consider the nanofluid saturating the porous medium as a "normal fluid", since the peculiar effects introduced in the model by Buongiorno [5] do not affect sensibly the numerical solution.

4. Conclusions

In the present paper, the steady laminar forced convection in a parallel-plane channel involving a nanofluid saturating a porous medium is studied. The flow is assumed to be fully developed, and described through the Brinkman's model. Downstream of an adiabatic preparation of the channel, a boundary temperature given by a linear function of the longitudinal coordinate is prescribed. A study of the thermal behaviour of the nanofluid is performed by solving numerically the fully elliptic governing equations. More precisely, the mathematical model proposed by Buongiorno [5] is employed, in order to evaluate the effects of thermophoresis and Brownian diffusion. In particular, the model yields to a pair of partial differential equations: one for the temperature field and one for the nanoparticle concentration distribution. The solution for the fully developed region is determined analytically, while the solution for the thermal entrance region is evaluated numerically by a Galerkin finite element method implemented through the software package Comsol Multiphysics (© Comsol, Inc.). The numerical solution is fairly independent of the dimensionless length of the channel, as well as of the mesh refinement.
The present analysis leads to the conclusion that thermophoresis and Brownian diffusion display negligible effects in realistic cases. In fact, the volumetric concentration of nanoparticle is a weak function of the temperature distribution, since it depends very weakly on the parameters γ and Pe. Moreover, both dimensionless temperature and nanoparticle concentration are weak function of the velocity distribution, since they depend very weakly on the parameter Λ as well. Indeed, the resolution of the fully-elliptic coupled equations, which arise from the model proposed by Buongiorno, requires a computational effort and yields to the determination of the nanoparticle concentration gradient, that may be neglected in many cases of practical interest.
A foreseen future development of the present analysis is to consider different boundary conditions, such as periodic boundary condition, since for the case of clear fluid the effect of Brownian diffusion and thermophoresis is not negligible for that boundary conditions.

References

[1] Choi S 1995 Enhancing thermal conductivity of fluids with nanoparticle, in D.A. Siginer, H.P. Wang, H.P. (Eds.), *Developments and Applications of Non-Newtonian Flows* ASME FED **231**/MD **66** ASME, New York 99
[2] Masuda H, Ebata A, Teramae K and Hishinuma N 1993 *Netsu Bussei* **4** 227
[3] Lee S, Choi SUS, Li S and Eastman JA 1999 *J. Heat Transfer* **121** 280
[4] Eastman JA, Choi SUS, Li S, Yu W and Thompson LJ 2001 *Appl. Phys. Lett.* **78** 718
[5] Buongiorno J 2006 *J. Heat Transfer* **128** 240
[6] Kakaç S amd Pramuanjaroenkij A 2009 *Int. J. Heat Mass Transfer* **52** 3187
[7] Wang XQ and Mujumdar AS 2007 *Int. J. Therm. Sci.* **46**1
[8] Daungthongsuk W and Wongwises S 2007 *Renew. Sust. Energ. Rev.* **11** 797
[9] Rao Y 2010 *Particuology* **8** 549
[10] Nield DA and Kuznetsov AV 2013 *J. Heat Transfer* **135** 061201

[11] Magyari E 2011 *Acta Mech.* **222** 381
[12] Tiwari R and Das M 2007 *Int. J. Heat Mass Transfer* **50** 2002
[13] Rossi di Schio E, Celli M and Barletta A 2014 *J. Heat Transfer* **136** 022401
[14] Nield DA and Kuznetsov AV 2014 *Int. J. Heat Mass Transfer* **70** 430
[15] Hung YM 2011 *Heat Transfer Eng.* **31**1184
[16] McNab GS and Meisen A 1973 *J. Colloid Interface Sci.* **44** 339